J Electroceram (2011) 27:109–113
DOI 10.1007/s10832-011-9653-8

Electrical characteristics of Cu-doped In_2O_3/Sb-doped SnO_2 ohmic contacts for high-performance GaN-based light-emitting diodes

Joon-Ho Oh · Tae-Yeon Seong · H.-G. Hong · Kyoung-Kook Kim · S.-W. Yoon · J.-P. Ahn

Received: 16 December 2010 / Accepted: 29 August 2011 / Published online: 14 September 2011

Abstract We characterized the electrical and chemical properties of Cu-doped In_2O_3(CIO) (2.5 nm thick)/Sb-doped SnO_2(ATO) (250 nm thick) contacts to p-type GaN by means of current-voltage measurement, scanning transmission electron microscope (STEM) and x-ray photoemission spectroscopy (XPS). The CIO/ATO contacts show ohmic behaviors, when annealed at 530 and 630°C. The effective Schottky barrier heights on diodes made with Ni (5 nm)/Au (5 nm) contacts decrease with increasing annealing temperature. STEM/energy dispersive x-ray (EDX) profiling results exhibit the formation of interfacial In-Ga-Sn-Cu-oxide. XPS results show a shift of the surface Fermi level toward the lower binding energy side upon annealing. Based on the STEM and XPS results, the ohmic formation mechanisms are described and discussed.

J.-H. Oh · T.-Y. Seong (✉)
Department of Materials Science and Engineering,
Korea University,
Seoul 136-713, South Korea
e-mail: tyseong@korea.ac.kr

H.-G. Hong
Material & Device Center,
Samsung Advanced Institute of Technology,
Suwon 440-600, South Korea

K.-K. Kim
Department of Nano-Optical Engineering,
Korea Polytechnic University,
Gyeonggi 429-793, South Korea

S.-W. Yoon · J.-P. Ahn
Advanced Analysis Center,
Korea Institute of Science and Technology,
Seoul 136-791, South Korea

Keywords Light emitting diode · Transparent electrode · SnO_2 · Ohmic contact

1 Introduction

High-performance GaN-based light-emitting diodes (LEDs) are of significant importance for solid-state lighting application [1]. To use LEDs as a solid-state lighting source, the external quantum efficiency (EQE) should be greatly improved. One of the ways to attain high EQE is to develop highly transparent and low-resistance ohmic contacts to p-type GaN [2–4]. Transparent conducting oxides (TCOs) have been considered as electrodes for p-GaN [5]. In order for TCOs to be effective electrodes for p-GaN, they should have low sheet resistance to cause uniform current spreading (and so uniform emission throughout the entire active area of LEDs), low contact resistivity to enhance carrier injection, and high transparency (at least 80% at visible wavelengths) to increase light extraction. Among various TCOs, indium tin oxide (ITO)-based electrodes have been most commonly used[6, 7], because of their good electrical and optical properties. There are, however, some drawbacks for ITO, such as thermal instability and shortage of indium [8, 9].

SnO_2-based TCOs have been extensively investigated [10] as potential transparent electrodes, which are expected to replace ITO electrodes because of their chemical and thermal stability and cheap cost. For example, doped SnO_2-based TCOs have been used as front contact materials for superstrate-structured thin-film solar cells and organic light-emitting diodes [11, 12]. Among various deposition methods, pulsed-laser deposition (PLD) is advantageous because it is a simple deposition system. Moreover, PLD generates highly energetic particles, allowing good film

quality and good adhesion to substrate [13, 14]. Recently, Hong et al. [15], investigating PLD Sb-doped SnO_2 (ATO) ohmic contacts to p-GaN, showed that LEDs fabricated with ATO (250 nm thick) combined with a Cu-doped In_2O_3 (CIO)(2.5 nm thick) interlayer produced much higher output power compared to LEDs with conventional Ni/Au contacts. However, ohmic formation mechanisms for the CIO/ATO p-contacts have not been clearly demonstrated so far. Thus, in this work, we have investigated the possible ohmic mechanisms of CIO/ATO contacts using scanning transmission electron spectroscopy (STEM) and x-ray photoemission spectroscopy (XPS) results. It is shown that the effective Schottky barrier heights (SBHs) decrease with increasing annealing temperature. Based on the STEM and XPS results, the ohmic formation mechanisms are described.

2 Experimental

A metalorganic chemical vapour deposition system was used to grow InGaN/GaN-based LED structures on a (0001) sapphire substrate. The LED structure consisted of a 30-nm-thick GaN nucleation layer, an undoped GaN layer (2 μm-thick), a 2.5-μm-thick Si-doped n-GaN layer, an active region (80 nm thick) (InGaN/GaN multi-quantum wells), a 0.12-μm-thick Mg-doped p-GaN layer (with a carrier concentration of $\sim 5\times10^{17}$ cm^{-3}). The samples were ultrasonically degreased using acetone, methanol and deionized (DI) water for 5 min per step, followed by N_2-blowing. To remove native oxide at the surface, the samples were dipped in a buffered oxide etch (BOE) solution for 20 min, followed by DI water rinsing and N_2 drying. Prior to electrode deposition, the samples were dipped in a BOE solution again for 1 min followed by DI water rinsing and N_2 blowing. Then, 2.5-nm-thick Cu-doped In_2O_3(CIO) layers were e-beam evaporated at room temperature. This was followed by the PLD growth of 250-nm-thick Sb-doped SnO_2(ATO) films. Details about the PLD growth were described elsewhere [15]. Some of the samples were annealed at 530 and 630°C for 1 min in air.

For electrical characterization, current-voltage (I-V) measurements were performed using a parameter analyzer (HP 4155A). The chemical bonding states of CIO/ATO contacts were characterized by x-ray photoemission spectroscopy (XPS)(PHI 5800 ESCA System) which were performed using an Al K_α (1486.6 eV) x-ray source in an ultrahigh vacuum chamber. C*1s* peak (284.6 eV) was used to calibrate XPS results. Scanning transmission electron microscope (STEM) examinations along with energy dispersive X-ray (EDX) profiling were performed to characterize the interfacial phases and the chemical states of the samples. The schematic cross-sectional view of a LED fabricated with a CIO/ATO electrode is shown in Fig. 1.

3 Results and discussion

It was shown that all the CIO(2.5 nm)/ATO(250 nm) contacts before and after annealing at 530 and 630°C exhibited linear I–V behaviors, as shown in Fig. 2 [ref. 15]. Notably, the electrical characteristics of the CIO/ATO contacts are significantly improved upon annealing at 530 and 630°C. For example, the CIO/ATO contacts showed the best electrical properties at 630°C, e.g., a specific contact resistance of 2.1×10^{-3} Ωcm^2. It is noted that the ATO only contact exhibited higher resistance compared to the annealed CIO/ATO contacts. In order to understand the ohmic formation mechanisms of the annealed CIO/ATO contacts, the effective SBHs are measured by means of the Norde [16] and I–V [17, 18] methods. Schottky diodes were formed using Ni(5 nm)/Au(5 nm) contacts which were annealed at 530°C in air. For the Norde method, a Norde function, F(V), is plotted against V, as given below [16]

$$F(V) = \frac{V}{2} - \frac{kT}{q}\ln\left[\frac{I(V)}{A A^{**} T^2}\right] \quad (1)$$

where A is the contact area, A^{**} is the effective Richardson constant, defined by $A^{**} = \frac{4\pi q k^2 m_h^*}{h^3}$. The value of A^{**} was calculated to be 104 Acm^{-2} k^{-2} assuming the effective hole mass (m_h^*) of 0.8 m_e for the *p*-GaN [19]. The effective SBH (ϕ_b) is given as

$$\phi_b = F(V_{min}) + \frac{V_{min}}{2} - \frac{kT}{q} \quad (2)$$

where $F(V_{min})$ is the minimum value of F(V) and V_{min} is the corresponding voltage. Figure 3(a) shows a plot of $F(V)$

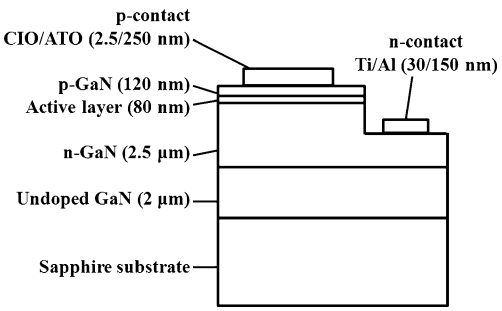

Fig. 1 The schematic and cross-sectional view of a LED fabricated with a CIO/ATO electrode

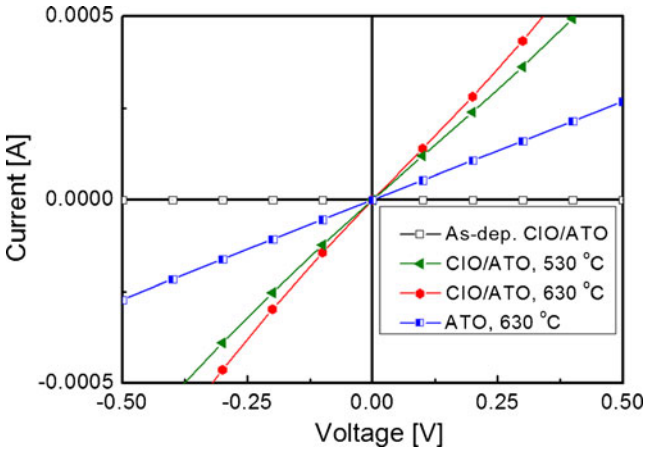

Fig. 2 Typical I–V characteristics of CIO/ATO p-contacts as a function of the annealing temperature

vs. *V* for the CIO/ATO contacts before and after annealing. The calculations show that the SBH is 0.77, 0.42 and 0.41 eV for the as-deposited, 530°C-annealed and 630°C-annealed samples, respectively. It is noted that the SBHs decrease with increasing annealing temperature.

To compare the SBHs, we also used the *I–V* method. [17, 18] Fig. 3(b) exhibits plots of $I/[1-\exp(-qV/kT)]$ vs. V for the CIO/ATO contacts before and after annealing. The measurements show that the SBHs are 0.74, 0.39 and 0.38 eV for the as-deposited, 530°C-annealed and 630°C-annealed samples, respectively. These values are smaller than those obtained by the Norde method. This might be attributed to the voltage dependence of SBHs [20], although the exact mechanism is not clearly understood at the moment.

To characterize the chemical bonding state of Ga, XPS examination was performed on the CIO/ATO samples on p-GaN before and after annealing at 630°C. Before commencing analyses, the contact layers were sputtered using Ar^+ ions to expose the interface region between the contact and GaN. Figure 4 shows the Ga 2*p* core level for the contact/GaN interface regions before and after annealing at 630°C. XPS core-level peak fittings were performed with a Shirley-type background and Lorentzian–Doniac–Sunsic curves convoluted with Gaussian profiles. Evidently, the Ga *2p* core level for the annealed sample shifts toward the lower energy side by 0.2 eV compared to the as-deposited sample. This indicates that the surface Fermi level shifts toward the valence band maximum and hence a reduction in the band-bending in p-type material [21]. This is consistent with the temperature dependence of the SBHs as measured by the Norde and I-V methods.

Figure 5(a) shows a Z-contrast STEM image together with a high-resolution TEM image obtained from the CIO/ATO sample annealed at 630°C. The STEM and HRTEM results reveal the presence of an interfacial layer whose thickness is in the range of 2.5 – 5 nm. The composition of the interfacial layer was characterized by means of EDX spectroscopy, as shown in Fig. 5(b). The EDX result showed that the interfacial layer consists of In, Ga, Sn,

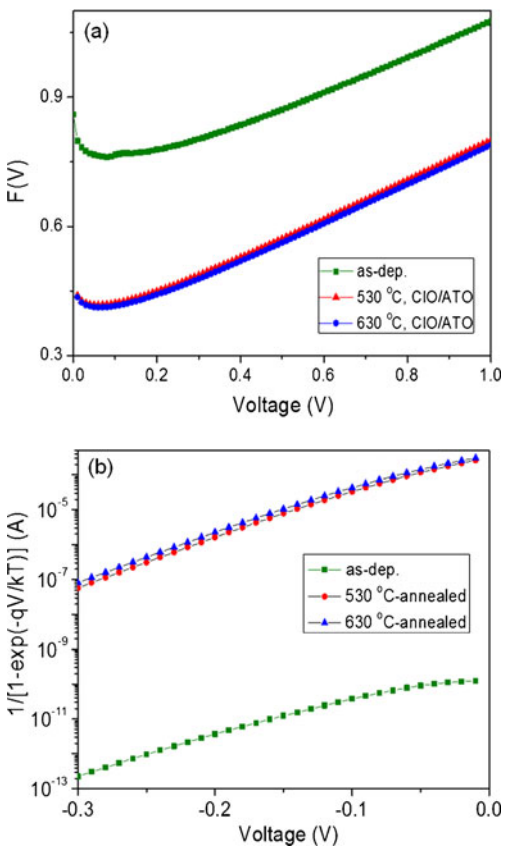

Fig. 3 (**a**) A plot of $F(V)$ vs. V for the CIO/ATO contacts before and after annealing. (**b**) Plots of I/[1-exp (-qV/kT)] vs. V for the CIO/ATO contacts before and after annealing

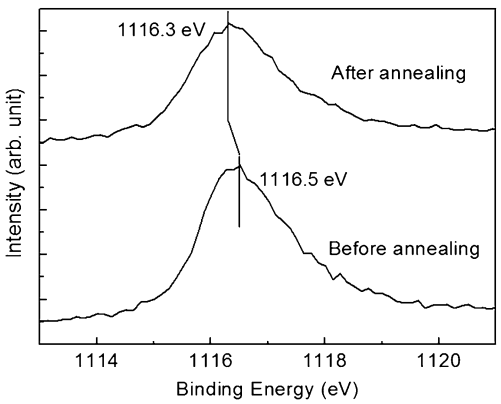

Fig. 4 The Ga *2p* core level for the contact/GaN interface regions before and after annealing at 630°C

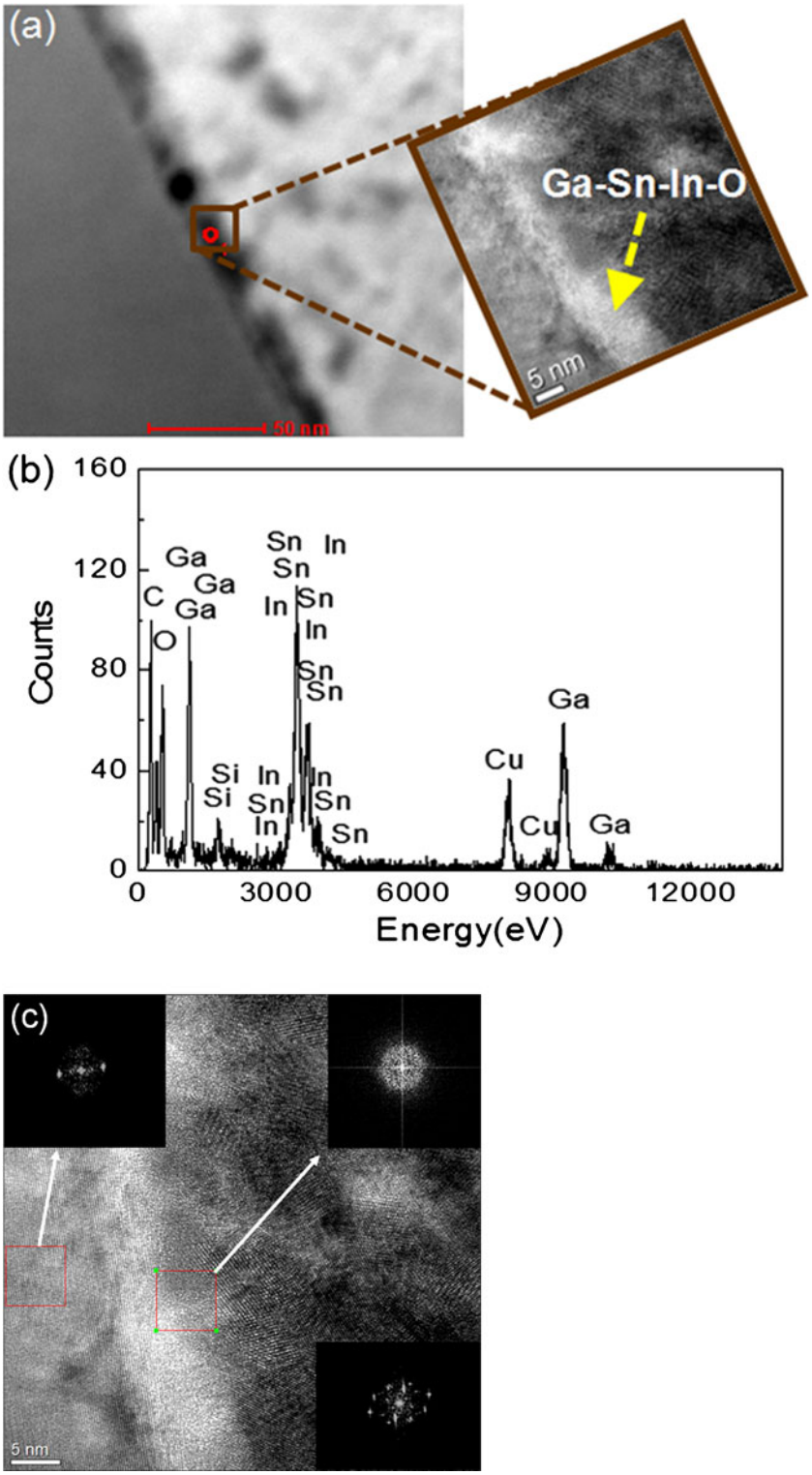

Fig. 5 (**a**) A Z-contrast STEM image together with a high-resolution TEM image obtained from the CIO/ATO sample annealed at 630°C. (**b**) EDX spectroscopy results from the interfacial layer, indicating the formation of multi-component In-Ga-Sn-Cu oxide. (**c**) An enlarged high-resolution TEM image of Fig. 5(a) with the FFT patterns obtained from GaN, an interfacial layer, and ATO (the insets)

Cu and oxygen, indicating the formation of multi-component In-Ga-Sn-Cu oxide. The interfacial layer was further characterized by means of fast Fourier transform (FFT) pattern. Figure 5(c) shows an enlarged high-resolution TEM image of Fig. 5(a) with the FFT patterns, which were obtained from the GaN, the interfacial layer, and the ATO. The FFT patterns from the GaN and the ATO (top left and bottom right in Fig. 5(c), respectively) reveal diffraction spots, indicating the crystalline nature. This implies that the as-deposited amorphous ATO was transformed into crystalline one upon annealing at 630°C. The FFT pattern (top right in Fig. 5(c)) obtained from the

interfacial layer exhibits diffuse ring without diffraction spots, being indicative of the amorphous nature. The STEM, HRTEM, and FFT results imply that annealing causes some amount of Ga atoms to outdiffuse into the interface region. The STEM/EDX results are in good agreement with the Auger electron spectroscopy (AES) data [15].

Based on the XPS and TEM-EDX results, the annealing-induced improvement of the electrical properties of the CIO/ATO contacts can be explained as follows. First, the improvement is attributed to the fact that the as-deposited amorphous ATO and CIO films become conductive after annealing [15]. It is noted that the CIO films become conductive with a sheet resistance of ~26 Ω/sq upon annealing at 630°C, which is comparable to that (~24 Ω/sq) of a reference ITO film. Second, the improvement can be attributed to the outdiffusion of Ga atoms, as confirmed by the STEM-EDX result (Fig. 5(b)). The outdiffusion of Ga atoms generates acceptor-like Ga vacancies near the GaN surface region under the contacts.[22] This results in an increase in the carrier concentration at the surface region and thereby a reduction in the band-bending, leading to reduction in the SBHs [21], as confirmed by the results obtained by the Norde and I-V methods. Therefore, the combined effects of the two believe to be responsible for the ohmic behaviours of the annealed CIO/ATO contacts.

4 Summary

The annealing dependence of the electrical properties of Cu-doped In_2O_3(CIO)/Sb-doped SnO_2(ATO) contacts to p-GaN was investigated by means of STEM and XPS. Calculations showed that the effective SBHs decreased with an increasing in the annealing temperature. Based on the STEM/EDX profiling and XPS results, the ohmic formation mechanisms were described in terms of a lowering of SBHs and the formation of multi-component oxide.

Acknowledgments This work was supported by Manpower Development Program for Energy & Resources (MKE)(Grant no. 2008-E-AP-HM-P-16-0000), National Research Foundation of Korea grant through World Class University program (R33-2008-000-10025-0), and the Industrial Technology Development Program funded by the MKE, Korea.

References

1. S. Nakamura, M. Senoh, N. Iwasa, S. Nagahama, Appl. Phys. Lett. **67**, 1868 (1995)
2. Y. Narukawa, J. Narita, T. Sakamoto, K. Deguchi, T. Yamada, T. Mukai, Jap. J. Appl. Phys. **45**, L1084 (2006)
3. J.-O. Song, S. Kwak, Y. Park, T.-Y. Seong, Appl. Phys. Lett. **86**, 213505 (2005)
4. J.-S. Jang, I.-S. Chang, H.-K. Kim, T.-Y. Seong, S. Lee, S.-J. Park, Appl. Phys. Lett. **74**, 70 (1999)
5. J.-O. Song, J.-S. Ha, T.-Y. Seong, IEEE Trans. Electron Devices **57**, 42 (2010)
6. T. Margalith, O. Buchinsky, D.A. Cohen, A.C. Abare, M. Hansen, S.P. DenBaars, Appl. Phys. Lett. **74**, 3930 (1999)
7. S.-M. Pan, R.-C. Tu, Y.-M. Fan, R.-C. Yeh, J.-T. Hsu, IEEE Photonics Technol. Lett. **15**, 646 (2003)
8. T.J. Coutts, D.L. Young, X. Li, W.P. Mulligan, X. Wu, J. Vac. Sci. Technol. A **18**, 2646 (2000)
9. X. Jiang, F.L. Wong, M.K. Fung, S.T. Lee, Appl. Phys. Lett. **83**, 1875 (2003)
10. T. Minami, Semicond. Sci. Technol. **20**, S35 (2005)
11. P.D. Veneri, L.V. Mercaldo, C. Privato, Renew. Energy **33**, 42 (2008)
12. D. Vaufrey, M. Ben Khalifa, M.P. Besland, C. Sandu, M.G. Blanchin, V. Teodorescu, J.A. Roger, J. Tardy, Synth. Met. **127**, 207 (2002)
13. H. Kim, A. Pique, Appl. Phys. Lett. **84**, 218 (2004)
14. H.-G. Hong, J.-O. Song, S.-H. Kim, T. Lee, T.-Y. Seong, J. Electrochem. Soc. **153**, G922 (2006)
15. H.-G. Hong, J.-O. Song, H. Na, H. Kim, K.-K. Kim, T.-Y. Seong, Electrochem. Solid State Lett. **10**, H254 (2007)
16. H. Norde, J. Appl. Phys. **50**, 5052 (1979)
17. T. Mori, T. Kozawa, T. Ohwaki, Y. Taga, S. Nagai, S. Yamasaki, S. Asami, N. Shibata, M. Koike, Appl. Phys. Lett. **69**, 3537 (1996)
18. E.H. Rhoderick, R.H. Williams, *Metal-semiconductor contacts* (Clarendon, Oxford, 1988)
19. J.I. Pankove, S. Bloom, G. Harbeke, RCA Rev. **36**, 163 (1975)
20. A.B. McLean, Semicond. Sci. Technol. **1**, 177 (1986)
21. J.-S. Jang, T.-Y. Seong, J. Appl. Phys. **88**, 3064 (2000)
22. V.M. Bermudez, D.D. Koleske, A.E. Wickenden, Appl. Surf. Sci. **126**, 69 (1998)